High volumetric hydrogen density phases of magnesium borohydride at high-pressure: A first-principles study*

Fan Jing(范 靖), Bao Kuo(包 括), Duan De-Fang(段德芳), Wang Lian-Cheng(汪连城), Liu Bing-Bing(刘冰冰), and Cui Tian(崔 田)†

State Key Laboratory of Superhard Materials, College of Physics, Jilin University, Changchun 130012, *China*

(Received 12 December 2011; revised manuscript received 26 January 2012)

The previously proposed theoretical and experimental structures, bond characterization, and compressibility of $Mg(BH_4)_2$ in a pressure range from 0 to 10 GPa are studied by *ab initio* density-functional calculations. It is found that the ambient pressure phases of meta-stable $I4_1/amd$ and unstable P-3m1 proposed recently are extra stable and cannot decompose under high pressure. Enthalpy calculation indicates that the ground state of $F222$ structure proposed by Zhou *et al.* [2009 *Phys. Rev.* B **79** 212102] will transfer to $I4_1/amd$ at 0.7 GPa, and then to a P-3m1 structure at 6.3 GPa. The experimental $P6_122$ structure (α-phase) transfers to $I4_1/amd$ at 1.2 GPa. Furthermore, both $I4_1/amd$ and P-3m1 can exist as high volumetric hydrogen density phases at low pressure. Their theoretical volumetric hydrogen densities reach 146.351 g H_2/L and 134.028 g H_2/L at ambient pressure, respectively. The calculated phonon dispersion curve shows that the $I4_1/amd$ phase is dynamically stable in a pressure range from 0 to 4 GPa and the P-3m1 phase is stable at pressures higher than 1 GPa. So the $I4_1/amd$ phase may be synthesized under high pressure and retained to ambient pressure. Energy band structures show that they are both always ionic crystalline and insulating with a band-gap of about 5 eV in this pressure range. In addition, they each have an anisotropic compressibility. The c axis of these structures is easy to compress. Especially, the c axis and volume of P-3m1 phase are extraordinarily compressible, showing that compression along the c axis can increase the volumetric hydrogen content for both $I4_1/amd$ and P-3m1 structures.

Keywords: hydrogen storage material, metal borohydride, thermodynamic stability, dynamical stability

PACS: 61.50.Ks, 62.50.–p, 63.20.D–, 71.20.–b **DOI:** 10.1088/1674-1056/21/8/086104

1. Introduction

Discovery of environmental friendly and renewable energy resources to replace fossil fuels is a major research goal. Hydrogen generation, storage reservoirs, and fuel cells are viewed as viable candidates for the next generation of energy resources. Hydrides are thought to be the bases of efficient hydrogen reservoirs, because their hydrogen densities are much greater in density than gaseous or liquid hydrogen. Therefore, researching and understanding the high density hydrides as potential hydrogen storage materials has attracted much attention.[1−12]

Among hydrides, $Mg(BH_4)_2$ is a promising lightweight solid-state hydrogen storage material with a theoretical hydrogen capacity of 14.8 wt%. The structures of $Mg(BH_4)_2$ in ambient conditions have been widely studied due to their potential application in hydrogen storage.[13−21] The measured low temperature structure of $Mg(BH_4)_2$ contains 330 atoms in a primitive cell with hexagonal $P6_1$ symmetry (α-phase). Above 453 K, an irreversible polymorphic transformation to an orthorhombic ($Fddd$) β-phase has been observed.[13,14] However, the first-principles calculations confirmed that the $P6_1$ structure is dynamically unstable and the corresponding stable structure should have $P6_122$ symmetry.[20] In 2007, Li *et al.*[22] suggested experimentally that $Mg(BH_4)_2$ desorbed hydrogen at an extraordinarily high temperature and was actually irreversible. These are due to its poor kinetic property. Thus, to improve the hydrogenation and dehydrogenation properties of $Mg(BH_4)_2$, catalysts such as Ti, have been explored.[23,24] Ball-milling is often used for adding

*Project supported by the National Basic Research Program of China (Grant No. 2011CB808200), the National Natural Science Foundation of China (Grant Nos. 51032001, 11074090, 10979001, and 51025206), and the Funds for Changjiang Scholar and Innovative Research Team in University (Grant No. IRT1132).

†Corresponding author. E-mail: cuitian@jlu.edu.com

© 2012 Chinese Physical Society and IOP Publishing Ltd

a catalyst into the hydride to enhance the dehydrogenation. The local stress can exceed several gigapascals in this process, in which the structural transition of the hydrides may be induced.[25,26] On the other hand, high pressure experiment is an effective method of synthesizing hydrogen storage materials with high volumetric hydrogen densities (VHDs), because compressions on materials are usually accompanied by irreversible volume collapse. Therefore, a better understanding of important physical properties such as structural transformation, compressibility, and bonding properties under high pressure may shed light on the synthesis and modifications of new compounds with possible application to clean energy technologies. The irreversible phase transition of $Mg(BH_4)_2$ was observed above 2.5 GPa,[27] but many aspects of phase transition in $Mg(BH_4)_2$ are still unknown and remain to be solved for a better understanding of its high pressure behaviours.

In this work, for understanding the high pressure behaviours of $Mg(BH_4)_2$, its crystal structure, bond characterization, and compressibility under high pressure are systematically studied by using the plane-wave pseudopotential method in the generalized gradient approximation (GGA).

2. Computational method

In this work, *ab initio* pseudopotential plane-wave density functional method is used, which is implemented in the CASTEP code.[28] All the structural optimizations in this paper including the atomic positions and the lattice constants are performed by the BFGS algorithm proposed by Broyden, Fletcher, Goldfarb, and Shannon,[29] which provides a fast way of finding the lowest energy structure and the optimized cell. The optimization will not be finished until the forces on the atoms are less than 0.01 eV/Å (1 Å=0.1 nm) and all the stress components are less than 0.02 GPa. The tolerance in the self-consistent field calculations is 5×10^{-7} eV/atom. Exchange and correlation effects are described in the Perdew–Burke–Ernzerh scheme of the GGA.[30] The summation over the Brillouin zone is performed with weighted summation over wave vectors generated by the Monkhorst–Pack scheme.[31] Convergence tests give $0.04\times2\pi$ Å^{-1} grid spacing and 600-eV cutoff energy. With such a choice, the error bar of total energy is about 0.7 meV per atom. The elastic stiffness coefficient is evaluated from the linear relationship (Hooke's law) between the resultant stress and applied strain. The lattice dynamics is determined using the forces acting on the atoms in the supercell. The dynamical matrix is constructed from the appropriate set of displacements of the symmetry-nonequivalent atoms. The details of the direct method are presented elsewhere.[32,33]

3. Results and discussion

In 2006, Nakamori *et al.*[15] proposed the P-$3m1$ and $P2/c$ structures. But the P-$3m1$ structure is unstable at ambient pressure due to the imaginary phonon frequencies. In 2009, Voss *et al.*[18] presented a new meta-stable high-density (ρ = 1.01 g·cm^{-3}) tetragonal ($I4_1/amd$) stable structure at ambient conditions, which can be interpreted as a folded form of the low-density I-$4m2$ structure (ρ = 0.56 g·cm^{-3}), and it is able to be synthesized, similar to $Ca(BH_4)_2$,[34] by high pressure techniques. Especially, this structure of $Mg(BH_4)_2$ has extra high theoretical hydrogen volumetric density, which exceeds the ultimate goal of the U.S. Department of Energy (70 g/L). The $Fddd$ structure shown in Fig. 1(e) is not the β-phase, but it is a substituted crystal structure starting from orthorhombic ($Fddd$) $Ca(BH_4)_2$.[35] For constructing the P-$4m2$ $Mg(BH_4)_2$, we proposed an alternative approach starting from the prototype structures of β-$NaBH_4$ with the $P42_1c$ symmetry.[36] Evidently, the ABH_4 model cannot be directly used due to the difference in stoichiometry, where A denotes metallic elements. To resolve this problem, we deduct a metallic atom in the body centre of the unit cell of ABH_4, thereby producing a modified structure. All the candidate $Mg(BH_4)_2$ structures are shown in Fig. 1. The structures with $F222$ symmetry proposed by both Voss *et al.* and Zhou *et al.* are not the same structures, but they are enantiomers approximately. We recall the $F222$ structure proposed by Voss *et al.* $F222$ (jpcm).

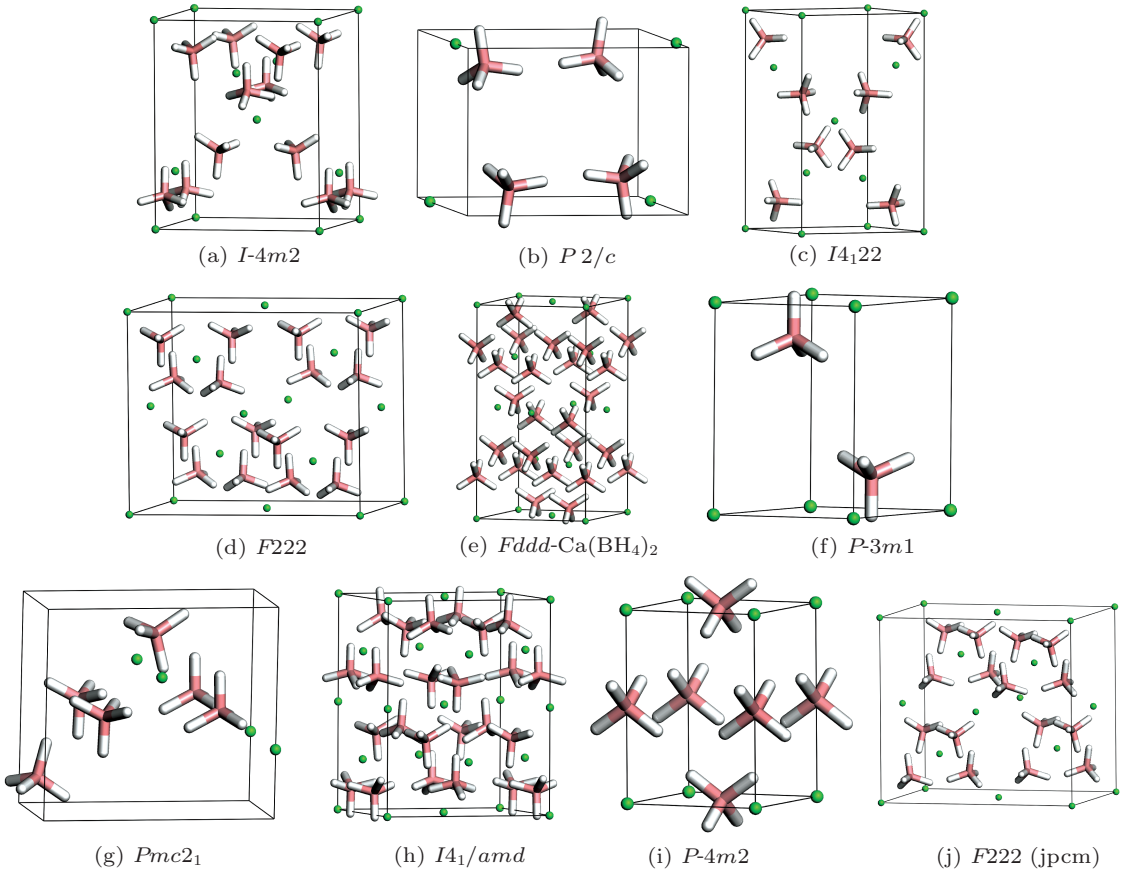


Fig. 1. (colour online) Candidate structures of $Mg(BH_4)_2$: (a) I-4m2, (b) $P2/c$, (c) $I4_122$, (d) $F222$, (e) $Fddd$-$Ca(BH_4)_2$, (f) P-3m1, (g) $Pmc2_1$, (h) $I4_1/amd$, (i) P-4m2, (j) $F222$ (jpcm).

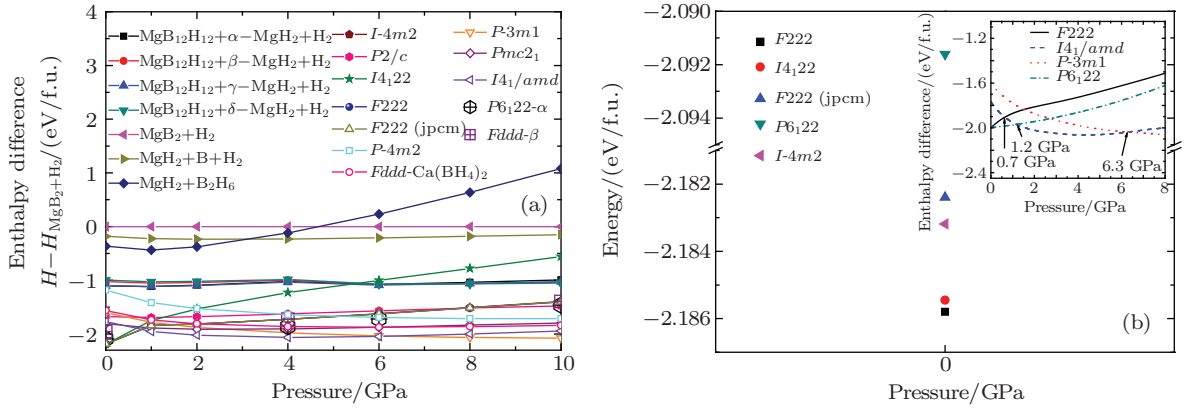


Fig. 2. (colour online) (a) Theoretical and experimental enthalpy-pressure curves of all the structures and seven possible decomposing paths. (b) Energies of $F222$, $I4_122$, $F222$ (jpcm), $P6_122$, and I-4m2 $Mg(BH_4)_2$ at ambient pressure. The insert shows enthalpy–pressure curves of $P6_122$, $F222$, $I4_1/amd$, and P-3m1 $Mg(BH_4)_2$ and phase transition points.

Various research groups attempted to identify the reaction path and intermediate products of the decomposition reaction of $Mg(BH_4)_2$.[22,24,37–44] A three-step reaction[24,40] was suggested as follows:

$$\begin{aligned} Mg(BH_4)_2 &\rightarrow MgH_2 + 2B + 3H_2 \\ &\rightarrow Mg + 2B + 4H_2 \\ &\rightarrow MgB_2 + 4H_2, \end{aligned}$$

where the last step is observed only when temperature is increased above 850 K. In addition, V. Ozolins *et al.*[45] proposed a reversible reaction with only 293 K of dehydrogenation temperature, which is as follows:

$$6Mg(BH_4)_2 \rightarrow MgB_{12}H_{12} + 5MgH_2 + 13H_2.$$

Therefore, in order to check the thermodynamic stability, we compare the enthalpies each as a function

of pressure for all the theoretical structures proposed by recent researches with MgB_2+4H_2, MgH_2+B_2H_6, $MgB_{12}H_{12}$+5MgH_2+13H_2, and MgH_2+2B+3H_2 as shown in Fig. 2(a). This figure indicates that all of these structures do not decompose below 10 GPa, which is in agreement with George *et al.*'s experimental results.[27] In these enthalpy calculations, α-B,[46,47] α-MgH_2, β-MgH_2, γ-MgH_2, δ-MgH_2,[48] β-B_2H_6,[49] AlB_2-type MgB_2, and the $P6_3/m$ hydrogen[50] are used. According to Fig. 2(a), only $I4_1/amd$ and P-3m1 structures are most stable in terms of thermodynamics under high pressure. According to our calculations, the energy order of the under debate ground states at ambient pressure is $F222$ < $I4_122$ < I-4m2 < $F222$ (jpcm) < $P6_122$ as shown in Fig. 2(b). The ground state with $F222$ symmetry proposed by Zhou *et al.*[19] will transform to a $I4_1/amd$ structure at 0.7 GPa, and then to a P-3m1 structure at 6.3 GPa. The $P6_122$ phase (α-phase) transforms to $I4_1/amd$ phase at 1.2 GPa as shown in the inset of Fig. 2(b). Therefore, both of the $I4_1/amd$ and P-3m1 structures are thermodynamically stable at high pressure and may be synthesized by high pressure experiments. It is noteworthy that there are 31.35% and 18.88 % of volume collapse from $Fddd$ and $P6_122$ to $I4_1/amd$ $Mg(BH_4)_2$, respectively. And the phase transition from $I4_1/amd$ to P-3m1 also has a volume collapse of 7.17% as shown in Fig. 3. The structural parameters, densities, and VHDs of all candidate structures are listed in Table 1 and compared with previous results. Each of these two stable phases has an extra high VHD. The theoretical VHDs reach 146.351 g H_2/L for $I4_1/amd$ and 134.028 g H_2/L for P-3m1 at ambient pressure, respectively.

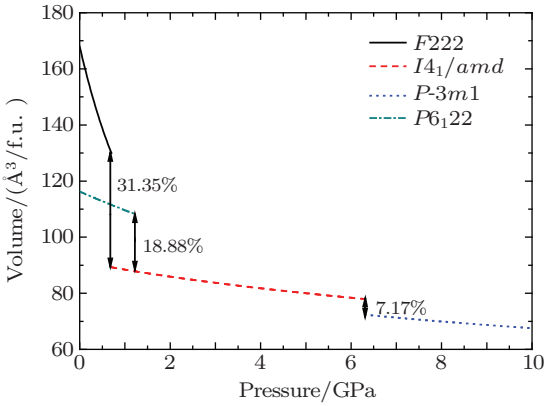


Fig. 3. (colour online) Volume differences among $P6_122$, $F222$, $I4_1/amd$, and P-3m1 $Mg(BH_4)_2$.

Table 1. Structural parameters (a, b, and c in unit Å), densities (ρ in unit g/cm^3), and VHDs (in g H_2/L) of all structures compared with previous results.

Space group	a	b	c	ρ	VHD	Ref.
$P6_122$	10.354	10.354	37.055	0.782	116.749	[20]
	10.478	10.478	37.057	0.763	113.996	[21]
	10.422	10.422	37.073	0.771	115.174	present work
$Fddd$	37.07	18.65	10.91	0.761	113.600	[13]
	36.90	18.83	10.65	0.775	115.792	[20]
	39.344	18.136	10.987	0.732	109.296	present work
$F222$	12.122	10.362	10.741	0.532	77.388	[19]
	12.111	10.359	10.728	0.533	79.579	present work
$F222$ (jpcm)	9.928	11.183	11.891	0.543	81.129	[18]
	9.996	11.234	11.931	0.535	79.942	[21]
	9.969	11.219	11.926	0.538	80.300	present work
$I4_122$	7.448	7.448	12.150	0.532	79.456	[19]
	7.449	7.449	12.151	0.532	79.429	present work
I-4m2	8.180	8.180	9.965	0.538	80.316	[17]
	8.186	8.186	9.980	0.536	80.078	[21]
	8.186	8.186	9.973	0.537	80.134	present work
$Pmc2_1$	4.3086	6.0878	8.3888	0.815	121.691	[16]
	4.321	8.131	8.128	0.628	93.765	[21]
	4.3334	6.6641	8.2997	0.748	111.702	present work
$I4_1/amd$	8.252	8.252	10.474	1.005	150.170	[18]
	8.317	8.317	10.580	0.980	146.351	present work
$P2/c$	6.777	5.552	8.085 β=75.40°	0.609	90.958	[15]
	6.767	5.833	7.726 β=79.58°	0.595	88.862	present work
P-3m1	4.279	4.279	5.761	0.981	146.559	[15]
	4.272	4.272	6.510	0.871	130.122	[21]
	4.263	4.263	6.347	0.897	134.028	present work
P-4m2	4.194	4.194	4.874	1.046	156.165	present work
$Fddd$-$Ca(BH_4)_2$	8.710	12.900	6.833	0.934	139.507	present work

The structural stabilities of ionic compounds often depend on their bonding properties and interactions between anions and ions. Thus, to understand the thermodynamic stability of $Mg(BH_4)_2$ under high pressure where no decomposition takes place, we analyse its bonding properties in a pressure range from 0 GPa to 10 GPa according to its calculated energy band structure as shown in Figs. 4(a)–4(d). The $I4_1/amd$ (Fig. 4(a) is for 0 GPa, Fig. 4(b) for 10 GPa), and P-3m1 $Mg(BH_4)_2$ (Fig.4(c) is for 0 GPa and Fig. (d) for 10 GPa) have similar band structures. Their conduction bands are all composed of 3s and 3p orbitals of Mg and B and 2s orbital of H. The valence bands are composed of sp^3 hybrid orbital in $[BH_4]^-$, and divided into two parts. The part composed of 1s of H and 2p of B has higher energy than the other part composed of 1s of H and 2s of B, and near to Fermi level. But the 2s band of Mg shows a straight line and no broadening, implying that the corresponding orbital does not contribute to bond. According to the energy band structure and the above analysis, both of these structures of $Mg(BH_4)_2$ are ionic crystalline and composed of Mg^{2+} and $[BH_4]^-$. All the 3s electrons of Mg transfer to B and contribute to an sp^3 hybrid orbital, so the 3s band of Mg is above the Fermi level and forms the conduction band. The 2s and 2p orbitals of B obtain these electrons and form sp^3 hybrid orbital, so the 2s and 2p band of B both are below the Fermi level and form valence band. Comparing Figs. 4(a)–4(d), there is no obvious change in band structure, showing that these bonding properties have not been changed in a pressure range of 0 GPa–10 GPa. Their band-gaps are always about 5 eV, showing that they are always insulators in this pressure range. The stabilities of these two structures under high pressure should be ascribed to this stable bonding nature.

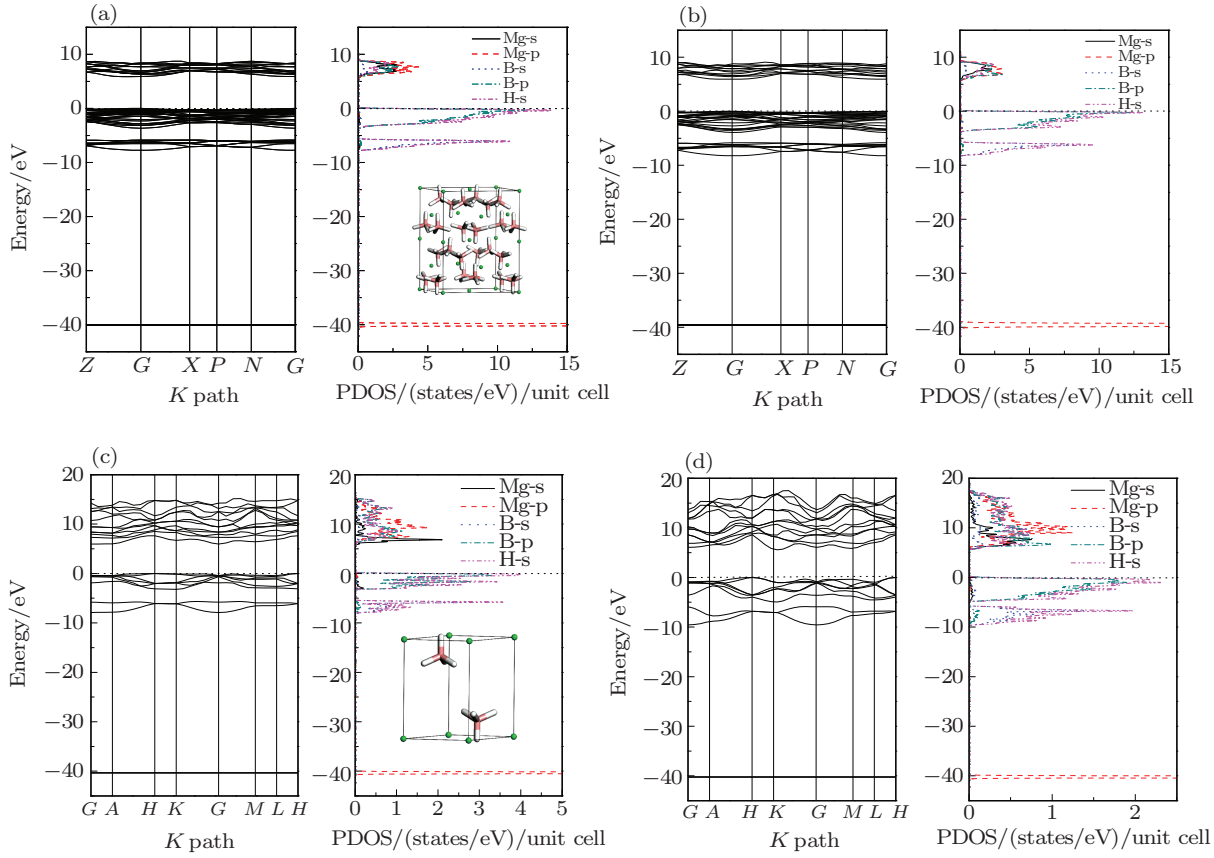


Fig. 4. (colour online) Energy band structures and partial densities of states of $I4_1/amd$ ((a) and (b)) and P-3m1 $Mg(BH_4)_2$ ((c), and (d)) at 0 GPa and 10 GPa, respectively.

The mechanical stability of structure provides a useful insight into crystal. The mechanical stability of a crystal requires the strain energy to be positive, which implies that the whole set of elastic constants C_{ij} satisfy Born–Huang criterion (the matrix of elastic constants C_{ij} must be positive-definite, i.e., the order principal minor determinants must be positive).[51] The formulas of elastic modulus for cubic, orthorhom-

bic, hexagonal, and monoclinic crystals are shown in Refs. [52]–[56]. The six calculated independent elastic constants of the $I4_1/amd$ structure at 6 GPa and eight independent elastic constants of the P-3m1 structure at 10 GPa are all listed in Table 2. They all satisfy the Born–Huang criterion, i.e., the $I4_1/amd$ and P-3m1 structure are both mechanical stable. The difference between C_{11} and C_{33} shows that they each have an anisotropic compressibility. Their c axes are all easy to compress compared with a and b axes. The small C_{66} of $I4_1/amd$ shows that it is easy to deform under the action of shear force on xz-plane and along x axis. The dynamical instability of $I4_1/amd$ $Mg(BH_4)_2$ above 5 GPa is related to this small stiffness. Details are discussed in the following part.

Table 2. Elastic constants (C_{ij} in unit GPa) of $I4_1/amd$ and P-3m1 structures calculated at 6 GPa and 10 GPa, respectively.

Space group	C_{11}	C_{33}	C_{44}	C_{66}	C_{12}	C_{13}	C_{14}	C_{24}
$I4_1/amd$	88.50	66.92	19.38	4.21	27.02	37.45		
P-3m1	104.84	76.44	21.09	26.00	52.84	46.86	–5.41	5.41

To check the dynamical stabilities of $I4_1/amd$ and P-3m1 phase at high pressure, we calculate their phonon densities of states (PHDOSs) and dispersion curves at 0, 2, 4, and 5 GPa for $I4_1/amd$ phase and 0, 1, 2, 4, 6, 8, and 10 GPa for P-3m1 phase. Figures 5(a)–5(d) show the PHDOSs and dispersion curves of $I4_1/amd$ phase at 0 GPa and 5 GPa and those of P-3m1 phase at 0 and 10 GPa. There are imaginary modes neither for $I4_1/amd$ phase at 0, 2, and 4 GPa nor for P-3m1 phase at 1, 2, 4, 6, 8, and 10 GPa. However, there are small imaginary modes near the G point both for $I4_1/amd$ phase at 5 GPa and for P-3m1 phase at 0 GPa due to the soft acoustic modes as shown in Figs. 5(b) and 5(c). Thus, the $I4_1/amd$ phase starts to transform to P-3m1 phase at about 5 GPa. It is also confirmed that the $I4_1/amd$ phase is dynamically stable at pressures between 0 and 4 GPa, and the P-3m1 phase is dynamically stable at pressures above 1 GPa. From Figs. 5(a)–5(d), it is found that the PHDOSs of $I4_1/amd$ phase and P-3m1 phase each consist of three separate bands. The low frequency range (0 THz–25 THz) is due mainly to the motion of the magnesium and boron framework, the medium range (30 THz–40 THz) corresponds to libration modes of $[BH_4]^-$, and the narrow high frequency range (70 THz–80 THz) corresponds to B–H stretching vibrations. These phonon vibration natures have not obviously changed in this pressure range, showing the most stable bond nature.

The anisotropic compressibility is universal in most materials. Compression can increase the VHD of a hydrogen storage material effectively. To increase volumetric hydrogen content more effectively, compression along the high compressible axis is reasonable. Therefore, the anisotropy of compressibility of material is most important. We analyse the anisotropies of compressibility and bulk compressibility by comparing the derivatives of lattice constant and volume with respect to pressure, ratios a/a_0, c/c_0, and V/V_0 of $I4_1/amd$ and P-3m1 structures which vary with pressure, in which V_0, a_0, and c_0 are the volume constant and the lattice constants at ambient pressure. It is found that the c axes of these two structures are easy to compress. Especially, the c axis of P-3m1 structure has an extraordinarily large compressibility as shown in Fig. 6(a). This anisotropy of compressibility should come from anisotropies of inner electrostatic fields of Mg^{2+} and $[BH_4]^-$. The bulk compressibilities of P-3m1 and $I4_1/amd$ structures as shown in Fig. 6(b), indicate that the P-3m1 structure has a larger compressibility, which is attributed to the smaller density of P-3m1 structure and the small electrostatic interaction between ions. From the comparison of derivatives of lattice constants with respect to pressure as shown in Fig. 6(c), it is found that the c axis of P-3m1 structure is most easy to compress below 2 GPa, but the ratio of compression decreases fast with the pressure increasing. Therefore, the absolute value of derivative of volume of P-3m1 structure is extremely large when pressure is below 2 GPa, and increases quickly with pressure increasing. When the pressure is larger than 5 GPa, the absolute value of derivative of volume of P-3m1 structure is smaller than that of $I4_1/amd$ structure as shown in Fig. 6(d).

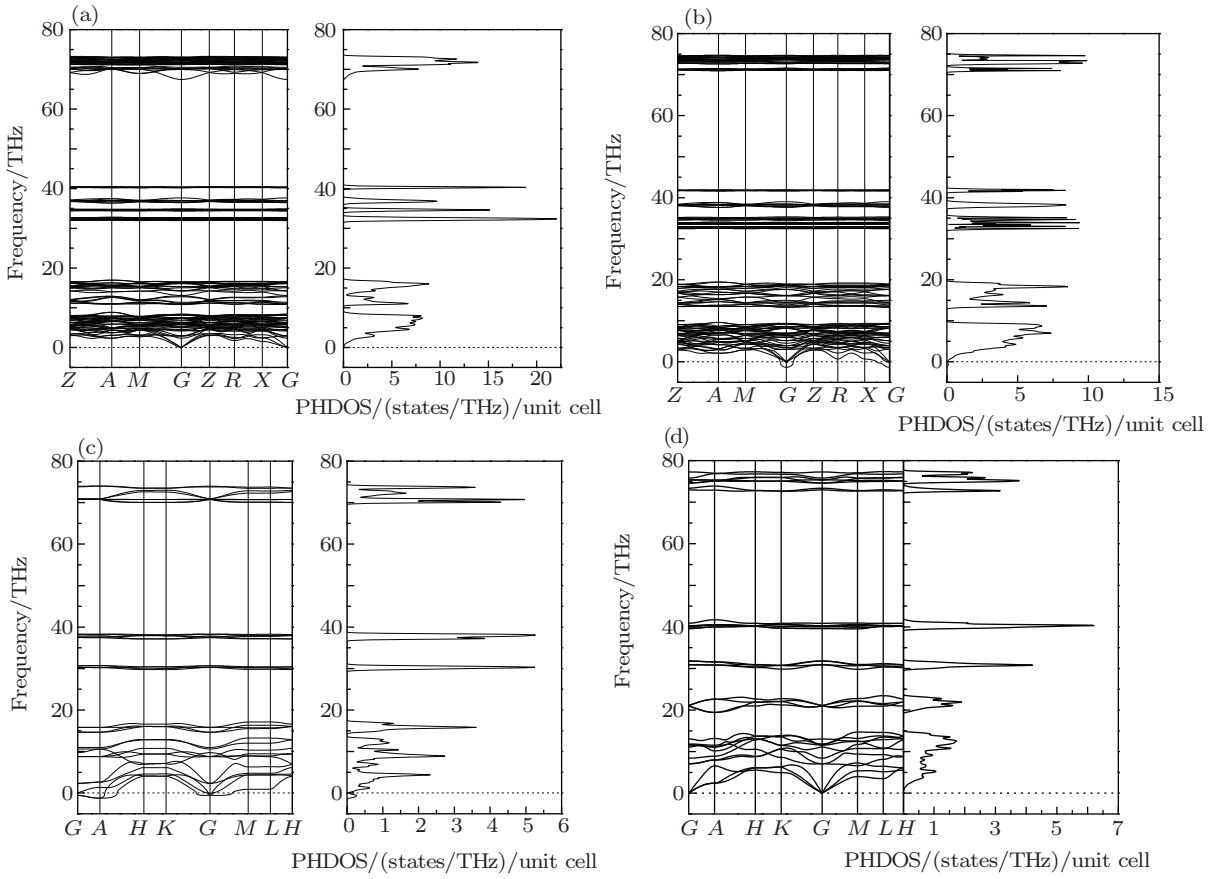


Fig. 5. Phonon dispersion curves and densities of states for $I4_1/amd$ at 0 GPa and 5 GPa ((a) and (b)) and P-3m1 at 0 GPa and 10 GPa ((c) and (d)), respectively.

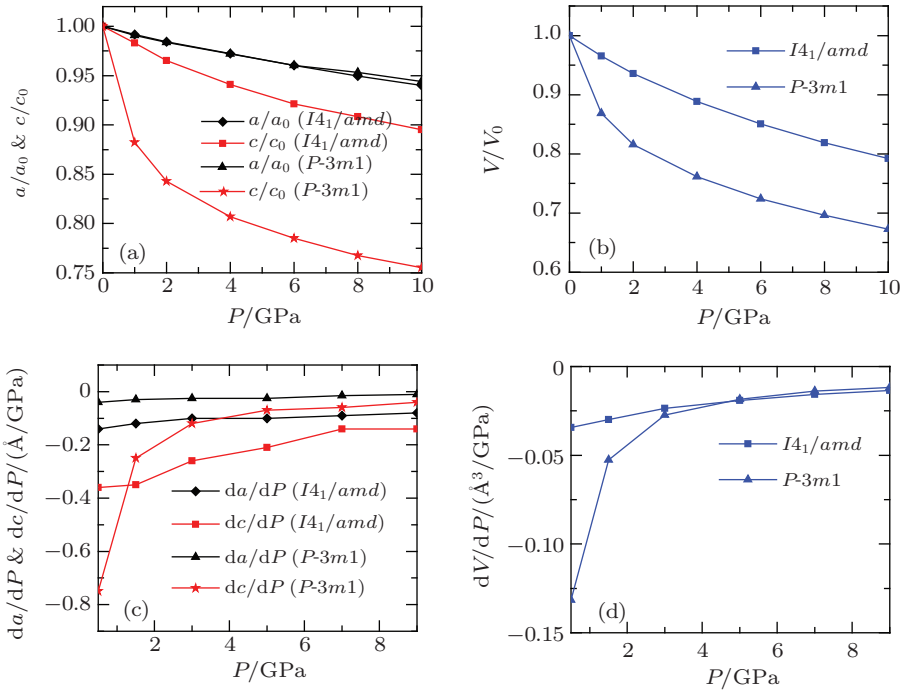


Fig. 6. (colour online) (a) Lattice constants of both $I4_1/amd$ and P-3m1 structures with respect to those at 0 GPa. (b) Volume of both $I4_1/amd$ and P-3m1 structures with respect to those at 0 GPa. (c) First derivatives of lattice constants of both $I4_1/amd$ and P-3m1 structures with respect to pressure. (d) First derivatives of volume of both $I4_1/amd$ and P-3m1 structures with respect to pressure.

4. Conclusion

In this paper, the high pressure (up to 10 GPa) behaviours of $Mg(BH_4)_2$ are investigated. Enthalpy calculation indicates that the ground state with $F222$ symmetry will transfer to $I4_1/amd$ at 0.7 GPa, and then to P-$3m1$ phase at about 5 GPa. And the experimental $P6_122$ structure (α-phase) transfers to $I4_1/amd$ at 1.2 GPa. Especially, there is a large volume collapse no matter whether the transfer takes place from $P6_122$ or $F222$ to $I4_1/amd$ phase due to its large VHD. The calculated elastic stiffness constants indicate that the $I4_1/amd$ and P-$3m1$ structures are both mechanical stable under high pressures. And the dynamical stability checking shows that the $I4_1/amd$ phase is stable in a pressure range from 0 GPa to 4 GPa and the P-$3m1$ phase is stable at pressures above 1 GPa. According to our calculation, it is predicted that the high hydrogen volumetric content structure of $I4_1/amd$ can be synthesized at high pressure experimentally and retained to ambient pressure, but the high compressible structure of P-$3m1$ can only exist as a high pressure phase. Furthermore, the anisotropies of compressibility and the bulk compressibility of $I4_1/amd$ and P-$3m1$ structures are analysed. It is found that the c axes of these structures are easy to compress. Especially, the c axis and volume of P-$3m1$ structure are extraordinarily compressible, showing that compression along the c axis can increase the volumetric hydrogen content for both $I4_1/amd$ and P-$3m1$ structures.

References

[1] Schlapbach L and Züttel A 2001 *Nature* **414** 353

[2] David E 2005 *J. Mater. Process. Technol.* **162** 169

[3] Lodziana Z and Vegge T 2004 *Phys. Rev. Lett.* **93** 145501

[4] Ravindran P, Vajeeston P, Fjellvåg H and Kjekshus A 2004 *Comput. Mater. Sci.* **30** 349

[5] Vajeeston P, Ravindran P, Vidya R, Fjellvåg H and Kjekshus A 2003 *Appl. Phys. Lett.* **82** 2257

[6] Vajeeston P, Ravindran P, Vidya R, Fjellvåg H and Kjekshusl A 2003 *Phys. Rev.* B **68** 212101

[7] Talyzin A V and Sundqvist B 2004 *Phys. Rev.* B **70** 180101

[8] Zhang H, Xiao M Z, Zhang G Y, Lu G X and Zhu S L 2011 *Acta Phys. Sin.* **60** 026103 (in Chinese)

[9] Wu D L, Xie A D, Wan H J and Ruan W 2011 *Acta Phys. Sin.* **60** 103101 (in Chinese)

[10] Ye X Q, Luo D L, Sang G and Ao B Y 2011 *Chin. Phys.* B **20** 017102

[11] Liu G L, Zhang G Y, Zhang H and Zhu S L 2011 *Chin. Phys.* B **20** 038801

[12] Ruan W, Xie A D, Yu X G and Wu D L 2011 *Chin. Phys.* B **20** 043104

[13] Her J H, Stephens P W, Gao Y, Soloveichik G L, Rijssenbeek J, Andrus M and Zhao J C 2007 *Acta Crystallogr. Sect.* B **63** 561

[14] Cerńy R, Filinchuk Y, Hagemann H and Yvon K 2007 *Angew. Chem.* **119** 5867

[15] Nakamori Y, Miwa K, Ninomiya A, Li H, Ohba N, Towata S, Züttel A and Orimo S I 2006 *Phys. Rev.* B **74** 045126

[16] Vajeeston P, Ravindran P, Kjekshus A and Fjellvåg H 2006 *Appl. Phys. Lett.* **89** 071906

[17] Ozolins V, Majzoub E H and Wolverton C 2008 *Phys. Rev. Lett.* **100** 135501

[18] Voss J, Hummelshøj J S, Łodziana Z and Vegge T 2009 *J. Phys.: Condens. Matter* **21** 012203

[19] Zhou X F, Qian Q R, Zhou J, Xu B, Tian Y J and Wang H T 2009 *Phys. Rev.* B **79** 212102

[20] Dai B, Sholl D S and Johnson J K 2008 *J. Phys. Chem.* C **112** 4391

[21] Caputo R, Tekin A, Sikora W and Züttel A 2009 *Chem. Phys. Lett.* **480** 203

[22] Li H W, Kikuchi K, Nakamori Y, Miwa K, Towata S and Orimo S I 2007 *Scr. Mater.* **57** 679

[23] Pinkerton F E, Meyer M S, Meisner G P and Balogh M P 2007 *J. Alloys Compd.* **433** 282

[24] Chlopek K, Frommen C, Leon A, Zabara O and Fichtner M 2007 *J. Mater. Chem.* **17** 3496

[25] Chellappa R S, Chandra D, Gramsch S A, Hemley R J, Lin J F and Song Y 2006 *J. Phys. Chem.* B **110** 11088

[26] Chellappa R S, Chandra D, Somayazulu M, Gramsch S A and Hemley R J 2007 *J. Phys. Chem.* B **111** 10785

[27] George L, Drozd V and Saxena S K 2009 *J. Phys. Chem.* C **113** 486

[28] Segall M, Lindan P, Probert M, Pickard C, Hasnip P, Clark S and Payne M 2002 *J. Phys.: Condens. Matter* **14** 2717

[29] Fischer T H and Almlof J 1992 *J. Phys. Chem.* **96** 9768

[30] Perdew J P, Burke K and Ernzerhof M 1996 *Phys. Rev. Lett.* **77** 3865

[31] Monkhorst H J and Pack J D 1976 *Phys. Rev.* B **13** 5188

[32] Computer code PHONON, Kraków, Poland, 2004

[33] Parlinski K, Li Z Q and Kawazoe Y 1997 *Phys. Rev. Lett.* **78** 4063

[34] Riktor M D, Sørby M H, Chłopek K, Fichtner M, Buchter F, Züttel A and Hauback B C 2007 *J. Mater. Chem.* **17** 4939

[35] Kim E, Kumar R, Weck P F, Cornelius A L, Nicol M, Vogel S C, Zhang J Z, Hartl M, Stowe A C, Daemen L and Zhao Y S 2007 *J. Phys. Chem.* B **111** 13873

[36] Miwa K, Aoki M, Noritake T, Ohba N, Nakamori N, Towata S, Züttel A and Orimo S 2006 *Phys. Rev.* B **74** 155122

[37] Matsunaga T, Buchter F, Mauron P, Bielman A, Nakamori Y, Orimo S, Ohba N, Miwa K, Towata S and Züttel A 2008 *J. Alloys Compd.* **459** 583

[38] Hanada N, Chlopek K, Frommen C, Lohstroh W and Fichtner M 2008 *J. Mater. Chem.* **18** 2611

[39] Hwang S J, Bowman R C, Reiter J W, Rijssenbeek J, Soloveichik G L, Zhao J C, Kabbour H and Ahn C C 2008 *J. Phys. Chem.* C **112** 3164

[40] Li H W, Kikuchi K, Nakamori Y, Ohba N, Miwa K, Towata S and Orimo S 2008 *Acta Mater.* **56** 1342

[41] Li H W, Miwa K, Ohba N, Fujita T, Sato T, Yan Y, Towata S, Chen W W and Orimo S 2009 *Nanotechnology* **20** 204013
[42] Li H W, Kikuchi K, Sato T, Nakamori Y, Ohba N, Aoki M, Miwa K, Towata I and Orimo S 2008 *Mater. Trans.* **49** 2224
[43] Ozolins V, Majzoub E H and Wolverton C 2009 *J. Am. Chem. Soc.* **131** 230
[44] Soloveichik G L, Gao Y, Rijssenbeek J, Andrus M, Kniajanski S, Bowman R C, Hwang S and Zhao J 2009 *Int. J. Hydrogen Energy* **34** 916
[45] Ozolins V, Majzoub E H and Wolverton C 2009 *J. Am. Chem. Soc.* **131** 230
[46] Will G and Kiefer B 2001 *Z. Anorg. Allg. Chem.* **627** 2100
[47] Oganov A R, Chen J H, Gatti C, Ma Y Z, Ma Y M, Glass C W, Liu Z X, Yu T, Kurakevych O O and Solozhenko V L 2009 *Nature* **457** 863
[48] Moriwaki T, Akahama Y and Kawamura H 2006 *J. Phys. Soc. Jpn.* **75** 074603
[49] Huebschle C B, Messerschmidt M, Lentz D and Luger P 2004 *Z. Anorg. Allg. Chem.* **630** 1313
[50] Pickard C J and Needs R J 2007 *Nat. Phys.* **3** 473
[51] Born M and Huang K 1956 *Dynamical Theory of Crystal Lattices* (Oxford: Clarendon)
[52] Haines J, Léger J M and Bocquillon G 2001 *Ann. Rev. Mater. Res.* **31** 1
[53] Watt J P 1979 *J. Appl. Phys.* **50** 6290
[54] Watt J P and Peselnick L 1980 *J. Appl. Phys.* **51** 1525
[55] Watt J P 1980 *J. Appl. Phys.* **51** 1520
[56] Wu Z J, Zhao E J, Xiang H P, Hao X F, Liu X J and Meng J 2007 *Phys. Rev.* B **76** 054115